JOURNAL OF COMPUTATIONAL PHYSICS 60, 263–281 (1985)

On the Stability of the Nonlinear Schrödinger Equation

B. M. HERBST*, A. R. MITCHELL†, AND J. A. C. WEIDEMAN*

*Department of Applied Mathematics, University of the Orange Free State, Bloemfontein 9300, South Africa

†Department of Mathematical Sciences, The University, Dundee DD1 4HN, Scotland, United Kingdom

Received March 28, 1984; revised August 27, 1984

The analytical and numerical stability properties of the nonlinear Schrödinger equation are investigated. It is shown how the analytical instabilities are reflected in semi- and fully discrete numerical schemes. Numerical results of nonlinear blowup and recurrence are given.

1. INTRODUCTION

One of the most serious difficulties encountered with the numerical solution of nonlinear time-dependent problems is known as "blowup." Typically this means that the numerical solution suddenly and usually with little warning becomes unbounded even if the analytical solution is known to be well behaved for all time. This phenomenon has been investigated for problems involving nonlinear terms of the form uu_x by Fornberg [8], Chin *et al.*, [3], Kuo Pen-Yu and Sanz-Serna [13], Griffiths [10], and Briggs *et al.*, [2], among others. For more general nonlinear terms very little seems to be known.

It is well known that the nonlinear Schrödinger equation (NLS)

$$iu_t + u_{xx} + q\,|u|^2 u = 0, \qquad i^2 = -1 \tag{1}$$

where q is a real parameter, is analytically unstable in the sense to be explained in Section 2 (see also Whitham [22], Stuart and Di Prima [21]). This is not uncommon among nonlinear dispersive waves in general and it plays an important part in the long time nature of the solution (see, e.g., Yuen and Ferguson [23]). This analytical instability also has important consequences for the numerical schemes used to solve nonlinear dispersive problems. Accordingly the main purpose of the present paper is to investigate some of the consequences of analytical instability for the numerical solution of the NLS. In particular we show how the analytical instability is reflected in various numerical schemes. We also show, mainly through numerical experiments, that the analytical instability may cause nonlinear blowup

0021-9991/85 $3.00

of the numerical scheme. However, a full or even a partial explanation of blowup for the NLS is not yet within our grasp. In fact, our analysis is based on a linearization and its applicability is therefore limited. For instance our analysis is not able to predict the long time behaviour of the solution and certainly gives no indication of the phenomenon of recurrence which will be discussed in Section 7.

In the next section we discuss the analytical stability properties of the NLS. In subsequent sections we investigate how the analytical instabilities are reflected in first a semi-discretised and then a fully discretised numerical scheme. In Section 5 we elaborate on the relationship between the analytical and numerical stability results. We then, in Section 6, give a numerical example illustrating one of the consequences of the numerical instability, namely blowup. The capability of our numerical methods to model recurrence is illustrated in Section 7. We conclude with a few general remarks concerning nonlinear instability.

2. Analytical Instability

Consider the linear dispersion equation

$$iu_t + u_{xx} = 0, \qquad i^2 = -1 \tag{2}$$

which has solutions of the form

$$u(x, t) = a \exp i(kx - wt) \tag{3}$$

where a is a complex constant and w satisfies the dispersion relation

$$w = k^2. \tag{4}$$

The NLS (1) also has solutions of the form (3), with the dispersion relation given by

$$w = D(k, a) := k^2 - q\,|a|^2. \tag{5}$$

The fact that (5) involves the wave number k as well as the amplitude a causes the solution to be unstable (Whitham [22, Sect. 14.2]). The instability can also be shown to exist by reasoning along similar lines as Stuart and Di Prima [21] and Whitham [22, Sect. 15.6]. Assume a solution of (1) of the form

$$u(x, t) = a \exp i(kx - D(k, a))\, t + \sigma(x, t). \tag{6}$$

Substitute (6) into (1) and assuming σ to be small, keep first-order terms in σ to obtain

$$i\sigma_t + \sigma_{xx} + qa^2 \exp[2i(kx - D(k, a)\, t)]\, \sigma^* + 2q\,|a|^2\, \sigma = 0 \tag{7}$$

where σ^* is the complex conjugate of σ. It is convenient to define $\varepsilon(x, t)$ by

$$\sigma(x, t) = a\varepsilon(x, t) \exp i(kx - D(k, a)\, t) \tag{8}$$

which enables us to write (6) in the form

$$u(x, t) = \exp iq\, |a|^2\, t\, z(x, t) \tag{9}$$

where $z(x, t)$ is given by

$$z(x, t) = a \exp i(kx - wt) + a\varepsilon(x, t) \exp i(kx - wt) \tag{10}$$

with w satisfying the dispersion relation (4). From (10) it is clear that $\varepsilon(x, t)$ can also be considered to be a perturbation of the solution (3) of the linear equation (2). Moreover, since $u(x, t)$ is a solution of (1), it follows from (9) that $z(x, t)$ satisfies

$$iz_t + z_{xx} - q\, |a|^2\, z + q\, |z|^2\, z = 0. \tag{11}$$

We return to these facts when we consider the stability of our numerical schemes.

To obtain the analytical stability results we assume σ to be given by

$$\sigma(x, t) = a(a_1(t) \exp i(k_1 x - D(k_1, a)\, t) + a_2(t) \exp i(k_2 x - D(k_2, a)\, t)) \tag{12}$$

where k_1 and k_2 satisfy the "resonance" condition

$$k_1 + k_2 = 2k. \tag{13}$$

Equation (13) will be satisfied if both the upper and lower side modes of k are present in (12), for example, if k_1 and k_2 are given by

$$k_1 = k + \mu, \qquad k_2 = k - \mu$$

for any value of μ.

Substituting (12) into (7) and making use of (13) yields the following equations for $a_1(t)$ and $a_2(t)$,

$$i\dot{a}_1 + q\, |a|^2\, a_1 + q\, |a|^2\, a_2^* \exp i\Omega t = 0 \tag{14a}$$

$$i\dot{a}_2 + q\, |a|^2\, a_2 + q\, |a|^2\, a_1^* \exp i\Omega t = 0 \tag{14b}$$

where

$$\Omega := D(k_1, a) - 2D(k, a) + D(k_2, a) = 2\mu^2.$$

From (14) it follows that a_1, a_2 satisfy

$$i\ddot{a}_j + \Omega\dot{a}_j - iq\, |a|^2\, \Omega a_j = 0, \qquad j = 1, 2$$

with solution

$$a_j = c_j \exp i\lambda_j t, \qquad j = 1, 2,$$

where λ_1, λ_2 satisfy

$$\lambda^2 - \Omega\lambda + q\,|a|^2\,\Omega = 0.$$

Thus, λ is complex and the perturbation $\sigma(x, t)$ grows exponentially in time whenever

$$q > 0, \qquad \mu^2 < 2q\,|a|^2. \tag{15}$$

The situation described by (15) is shown in Fig. 1. It is clear that all the lower modes ($\mu = 0$ excluded) are unstable with the exact number of unstable modes determined by the magnitude of the nonlinear contribution $q\,|a|^2$.

Of course, our analysis is only valid for a short time while the perturbation σ is still small. The long time behaviour of the solution is determined by various conservation laws such as

$$\frac{d}{dt}\int_{-\infty}^{\infty} |u(x, t)|^2\,dx = 0 \tag{16a}$$

and

$$\frac{d}{dt}\int_{-\infty}^{\infty} (|u_x(x, t)|^2 - \tfrac{1}{2}q\,|u(x, t)|^4)\,dx = 0. \tag{16b}$$

Making use of (16) it can be shown (Glassey [9], Strauss [20]) that the solution of (1) and its first derivative remains bounded in the L^2 norm for all time. The initial instabilities will therefore not grow indefinitely. One numerical example of the long-time behaviour of the solution is given in Section 7.

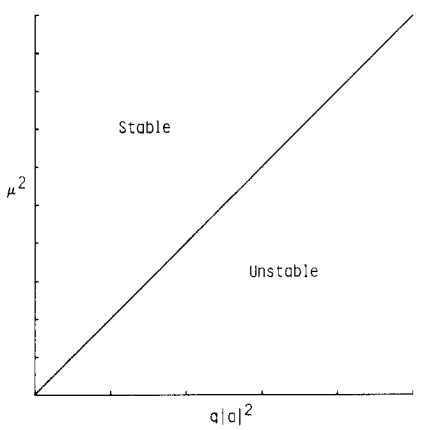

FIG. 1. Stability regions for the analytical solution.

3. Semi-Discretisations

We now consider

$$iu_t + u_{xx} + pu + q|u|^2 u = 0, \qquad i^2 = -1 \tag{17}$$

where p is a real parameter. The addition of the linear term pu in (17) allows us to obtain (11) by putting

$$p = -q|a|^2 \tag{18}$$

and also by putting $q = 0$ in (17) we can compare our results with those which are obtained from an analysis of a linearised version of (1).

In order to solve (17) numerically we follow Griffiths *et al.* [11], put

$$u(x, t) = v(x, t) + iw(x, t),$$

and rewrite (17) as the real system

$$\mathbf{u}_t + A\mathbf{u}_{xx} + pA\mathbf{u} + q\mathbf{f}(\mathbf{u}) = 0 \tag{19}$$

where

$$\mathbf{u} := (v, w)^T, \qquad A := \begin{pmatrix} 0 & 1 \\ -1 & 0 \end{pmatrix}, \qquad \mathbf{f}(\mathbf{u}) := (\mathbf{u}^T\mathbf{u})\, A\mathbf{u}.$$

The space variable in (19) is now discretised by using Galerkin's method with piecewise linear test and trial functions and product approximation (Christie *et al.* [4]) for the nonlinear term. Thus we obtain

$$M\dot{\mathbf{U}} + \frac{1}{h^2} S\mathbf{U} + pQ\mathbf{U} + qM\mathbf{F}(\mathbf{U}) = 0 \tag{20}$$

where a dot denotes the total derivative with respect to time, h is the uniform space discretisation and

$$M := \frac{1}{6}\begin{bmatrix} 2I & I & & 0 \\ I & 4I & I & \\ & \ddots & \ddots & \ddots \\ & I & 4I & I \\ 0 & & I & 2I \end{bmatrix}, \qquad S := \begin{bmatrix} -A & A & & 0 \\ A & -2A & A & \\ & \ddots & \ddots & \ddots \\ & A & -2A & A \\ 0 & & A & -A \end{bmatrix}$$

$$Q := \frac{1}{6}\begin{bmatrix} 2A & A & & & 0 \\ A & 4A & A & & \\ & \ddots & \ddots & \ddots & \\ & & A & 4A & A \\ 0 & & & A & 2A \end{bmatrix}, \qquad I := \begin{pmatrix} 1 & 0 \\ 0 & 1 \end{pmatrix}$$

$$\mathbf{U} := (\mathbf{U}_1, \ldots, \mathbf{U}_N)^T, \qquad \mathbf{U}_j := (V_j, W_j)^T$$

$$\mathbf{F} := (\mathbf{F}_1, \ldots, \mathbf{F}_N)^T, \qquad \mathbf{F}_j := (\mathbf{U}_j^T \mathbf{U}_j)\, A\mathbf{U}_j.$$

It should be pointed out that S simply represents a central difference replacement of the second derivative appearing in (1), when written as a system of two real-valued functions. M and Q arise from the use of the Galerkin method, M of course being the mass matrix.

If we now consider a perturbed solution of (20) of the form $\mathbf{U} + \boldsymbol{\delta}$, where $\boldsymbol{\delta}$ is assumed to be small, we find to first order in $\boldsymbol{\delta}$ that

$$M\dot{\boldsymbol{\delta}} + \frac{1}{h^2} S\boldsymbol{\delta} + pQ\boldsymbol{\delta} + qT\boldsymbol{\delta} = 0 \tag{21}$$

where

$$T := \frac{1}{6}\begin{bmatrix} 2B & B & & & 0 \\ B & 4B & B & & \\ & \ddots & \ddots & \ddots & \\ & & B & 4B & B \\ 0 & & & B & 2B \end{bmatrix}, \qquad B := \begin{pmatrix} 2vw & v^2 + 3w^2 \\ -(3v^2 + w^2) & -2vw \end{pmatrix},$$

the values in B being the local constant values of the solution of (19).

We now assume a solution of (21) of the form

$$\boldsymbol{\delta}_j(t) = \mathbf{d}(t) \exp i\alpha hj$$

to obtain

$$\gamma_t \dot{\mathbf{d}} - (4s^2/h^2)\, A\mathbf{d} + \gamma pA\mathbf{d} + \gamma qB\mathbf{d} = 0 \tag{22}$$

where

$$s := \sin \alpha h/2, \qquad \gamma_t = \gamma := 1 - \tfrac{2}{3}s^2.$$

Using

$$\gamma_t = 1, \qquad \gamma = 1 - \tfrac{2}{3}s^2$$

in (22) corresponds to mass lumping and apart from boundary conditions, the choice

$$\gamma_t = 1, \qquad \gamma = 1$$

implies the use of the finite difference scheme of Sanz-Serna and Manoranjan [19].

Rewriting (22) as

$$\dot{\mathbf{d}} = G\mathbf{d}$$

it follows that the eigenvalues, λ, of G satisfy

$$\det(\gamma_t \lambda I - (4s^2/h^2)\, A + \gamma p A + \gamma q B) = 0$$

or

$$\gamma_t^2 \lambda^2 = -\left(\frac{4s^2}{h^2} - \gamma p - 3\gamma q\, |a|^2\right)\left(\frac{4s^2}{h^2} - \gamma p - \gamma q\, |a|^2\right), \tag{23}$$

assuming δ is a perturbation on a constant modulus solution, i.e.,

$$|u|^2 = |a|^2.$$

For stability we require the eigenvalues to be imaginary which will be the case if

$$0 \leqslant \left(\frac{4s^2}{h^2} - \gamma p - 3\gamma q\, |a|^2\right)\left(\frac{4s^2}{h^2} - \gamma p - \gamma q\, |a|^2\right). \tag{24}$$

The stability regions given by (24) are shown in Fig. 2. From (24) and Fig. 2 it is clear that the linear term pu in (17) stabilizes the numerical scheme if $p > 0$. For instance, if

$$\gamma p \geqslant 4/h^2$$

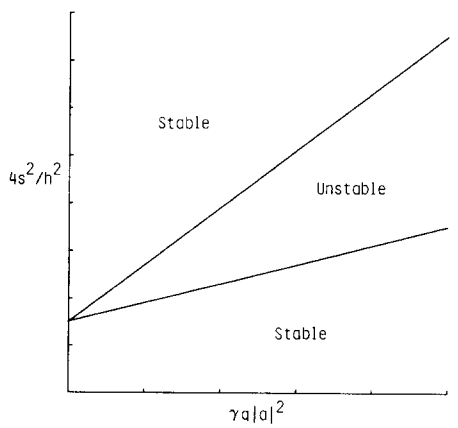

FIG. 2. Stability regions for the semi-discretised scheme.

then all modes α are stable for all values of the nonlinear contribution $\gamma q\,|a|^2$. It is also clear that no instability arises if the linear equation obtained from (17) with $q=0$ is used.

Finally we observe that the choice (18) in (24) implies that λ is real and the scheme unstable if

$$q>0, \qquad \frac{4s^2}{h^2}<2\gamma q\,|a|^2. \tag{25}$$

Equation (15) is obtained from (25) by letting $h\to 0$ with α playing the role of μ. We elaborate on this observation in Section 5.

4. Leapfrog Scheme

The time variable in (21) is now discretised by the leapfrog scheme (Mitchell and Morris [16]), to give

$$M\boldsymbol{\delta}^{n+1}-M\boldsymbol{\delta}^{n-1}+2rS\boldsymbol{\delta}^{n}+2\tau pQ\boldsymbol{\delta}^{n}+2\tau qT\boldsymbol{\delta}^{n}=0 \tag{26}$$

where τ is the time step and

$$r=\tau/h^2.$$

We assume a solution of (26) of the form

$$\boldsymbol{\delta}_j^n=\mathbf{d}^n\exp i\alpha hj$$

and define the amplification matrix, $\tilde{G}$, by

$$\mathbf{d}^{n+1}=\tilde{G}\mathbf{d}^n.$$

It now follows that the eigenvalues λ of $\tilde{G}$ satisfy

$$\det(\lambda^2\gamma_t I-\gamma_t I+(2\tau\gamma p-8rs^2)\,\lambda A+2\tau\gamma q\lambda B)=0$$

or

$$\gamma_t^2\lambda^4+2b\lambda^2+\gamma_t^2=0 \tag{27}$$

where

$$b:=-\gamma_t^2+2(4rs^2-\tau\gamma p-3\tau\gamma q\,|a|^2)(4rs^2-\tau\gamma p-\tau\gamma q\,|a|^2) \tag{28}$$

where we have again assumed that $\boldsymbol{\delta}$ is a perturbation on a constant modulus solution, i.e.,

$$|u|^2=|a|^2.$$

For stability we require

$$|\lambda| \leqslant 1$$

or equivalently from (27)

$$b^2/\gamma_t^4 \leqslant 1. \tag{29}$$

The stability condition now follows from (28) and (29) and is given by

$$0 \leqslant \left(\frac{4s^2}{h^2} - \gamma p - 3\gamma q\,|a|^2\right)\left(\frac{4s^2}{h^2} - \gamma p - \gamma q\,|a|^2\right) \leqslant \gamma_t^2/\tau^2. \tag{30}$$

The stability regions given by (30) are shown in Fig. 3.

Again we find that the choice (18) leads to (25). Equation (30) also imposes a restriction on the time step τ which for the linear dispersive equation (2) becomes

$$\tau \leqslant \tfrac{1}{4}\gamma_t h^2. \tag{31}$$

Finally we note that mass-lumping,

$$\gamma_t = 1,$$

increases the maximum value of the time step given by (31). On the other hand $\gamma = 1$ in (25) increases the range of unstable modes.

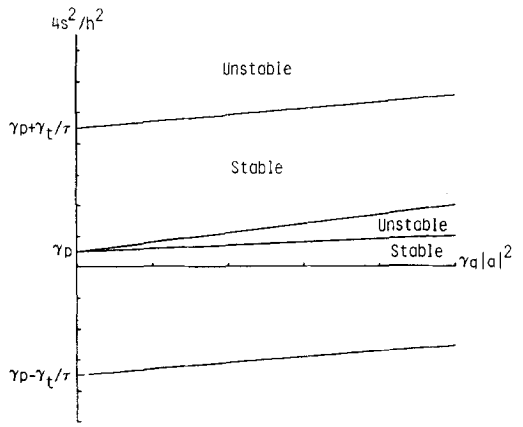

FIG. 3. Stability regions for the fully discretised scheme.

5. Relationship between Analytical and Numerical Stability

In the previous two sections we have seen that discrete analogues of the analytical result (15) may be obtained by using the choice (18) in (17). This result needs more explanation.

In Section 2 we obtained the analytical stability result by considering (11), i.e. (17) with p given by (18). We assumed the solution of (11) to be a perturbation of the linear equation (2), i.e., we assumed

$$z = l + \delta \tag{32}$$

where l is a solution of (2) and δ is small (cf. (10)). A specific choice for δ leads to (15).

Proceeding as in Section (3), the approximation $\mathbf{Z}$ of the solution of (11) satisfies

$$M\dot{\mathbf{Z}} + \frac{1}{h^2} S\mathbf{Z} - q\,|a|^2\, Q\mathbf{Z} + qM\mathbf{F}(\mathbf{Z}) = 0. \tag{33}$$

In order to follow the analytical arguments as closely as possible we now assume that

$$\mathbf{Z} = \mathbf{L} + \boldsymbol{\phi} \tag{34}$$

where $\boldsymbol{\phi}$ is small and $\mathbf{L}$ satisfies

$$M\dot{\mathbf{L}} + \frac{1}{h^2} S\mathbf{L} = 0 \tag{35}$$

with $\mathbf{L}_i^T \mathbf{L}_i = |a|^2$. From (33), (34), and (35) we obtain to first order in $\boldsymbol{\phi}$,

$$M\dot{\boldsymbol{\phi}} + \frac{1}{h^2} S\boldsymbol{\phi} + qR\boldsymbol{\phi} = 0 \tag{36}$$

where

$$R := \frac{1}{6}\begin{bmatrix} 2D & D & & 0 \\ D & 4D & D & \\ & \ddots & \ddots & \ddots \\ & D & 4D & D \\ 0 & & D & 2D \end{bmatrix}, \qquad D := 2\begin{pmatrix} vw & w^2 \\ -v^2 & -vw \end{pmatrix}$$

and v and w denote the real and imaginary parts respectively of the solution of (11).

Equation (36) may also be obtained by substituting (18) with $v^2 + w^2 = |a|^2$ into (21) which, as we have already observed, leads to the discrete analogue (25) of the analytical result (15).

Finally we observe a difference between the analytical and numerical stability results. In the numerical case we did not have to assume a special form of the perturbation as we did in the analytical analysis, cf. (13). From this we conclude that because of the discretisation, resonance will always take place in the numerical case. In this sense the numerical solution appears to be more unstable than its analytical counterpart.

6. Nonlinear Blowup

In order to illustrate the significance of the instability to the performance of our numerical schemes, we solve (1) by using the predictor–corrector scheme suggested by Griffiths *et al.*, [11]; i.e., we solve

$$M\mathbf{U}^* = M\mathbf{U}^n - rS\mathbf{U}^n - \tau q M\mathbf{F}(\mathbf{U}^n) \tag{37a}$$

$$\left(M + \frac{1}{2}rS\right)\mathbf{U}^{n+1} = \left(M - \frac{1}{2}rS\right)\mathbf{U}^n - \tau q M\mathbf{F}\left(\frac{\mathbf{U}^* + \mathbf{U}^n}{2}\right) \tag{37b}$$

where τ is the fixed time step and

$$r = \tau/h^2.$$

Griffiths *et al.*, [11] argued that it may sometimes be advantageous to consider the analogue of (37) as applied to

$$i\frac{du}{dt} + q\,|u|^2\,u = 0 \tag{38}$$

which is given by

$$\mathbf{U}^* = \mathbf{U}^n - \tau q\mathbf{F}(\mathbf{U}^n) \tag{39a}$$

$$\mathbf{U}^{n+1} = \mathbf{U}^n - \tau q\mathbf{F}\left(\frac{\mathbf{U}^* + \mathbf{U}^n}{2}\right). \tag{39b}$$

The energy at the nth time level, $|E_n|$, defined by

$$E_n^2 = \mathbf{U}^{n^T}\mathbf{U}^n$$

satisfies

$$E_{n+1}^2 = [1 + \tau^2 q^2 E_n^4(1 + \tfrac{1}{4}\tau^2 q^2 E_n^4)([1 + \tfrac{1}{4}\tau^2 q^2 E_n^4]^2 - 1)]\,E_n^2. \tag{40}$$

It is clear that (40) allows a slow growth in the energy at successive time levels which increases with increasing values of τq and E_n. Equation (38) is particularly

relevant if we solve the nonlinear Schrödinger equation (1) using the initial condition

$$u(x, 0) = A \tag{41}$$

where A is a complex constant. For this choice of initial condition the analytical solution of (1) is given by

$$u(x, t) = A \exp iq\,|A|^2\, t, \tag{42}$$

a solution which is independent of x. Also, (42) is in the form of the fundamental mode appearing in (6), with $k = 0$. Thus, if we solve (38) using the initial condition (41) we expect a slow increase in the energy according to (40). We also expect round-off error to introduce side modes which will then grow exponentially according to (25). Since our numerical scheme does not conserve the energy which would keep this exponential growth in hand, we anticipate unstable behaviour from our numerical solution.

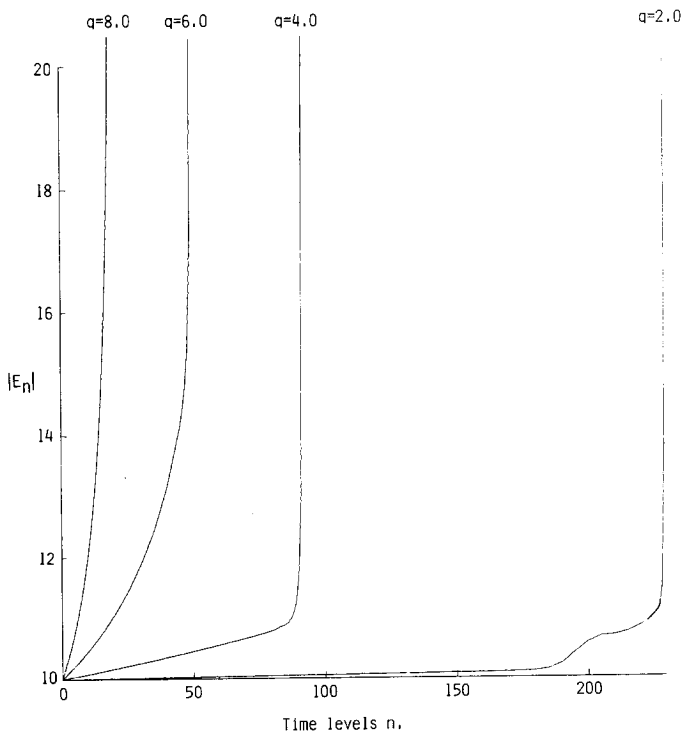

FIG. 4. The behaviour of the energy for various values of q.

The details of our numerical experiments are the following. We imposed natural boundary conditions at -5.0 and 5.0, i.e., we used

$$0 = u_x(-5.0, t) = u_x(5.0, t) \qquad \text{for all } t.$$

Using $A = 1.0$ in (41), $h = 0.5$, and $\tau = 0.05$, we solved (37) for $q = 2.0$, 4.0, 6.0, and 8.0. In Fig. 4 we plotted the energy E_n at the various time levels, n.

As predicted by (40) the energy grows at an increasing rate for increasing values of q. However, after a certain time, which decreases with increasing q, the energy becomes unbounded, i.e., its value overflows the computer. Although the actual blowup itself is not explained by any of the results in the previous sections, some insight in the underlying mechanism causing this to happen might be obtained from the following observation.

Accepting that for $q = 2.0$, the energy blows up after 230 steps, the transformation

$$\tau' = \tau q$$

would suggest a uniform decrease in blowup times for increasing values of q. This predicts blowup times of 115, 76, and 57 time steps for $q = 4.0$, 6.0, and 8.0, respectively. However the energy becomes unbounded after 92, 50, and 19 time steps.

7. Recurrence

For this numerical illustration we add a perturbation to the initial condition (41) containing side modes which satisfy the resonance condition (13). Accordingly we consider

$$u(x, 0) = A + \sigma(x, 0) \tag{43a}$$

where

$$\sigma(x, 0) = A(a_1(0) \exp(i\mu x) + a_2(0) \exp(-i\mu x)). \tag{43b}$$

It is clear that (43b) is of the form (12) with

$$k = 0, \qquad k_1 = \mu, \qquad k_2 = -\mu.$$

According to (15) the perturbation (43b) will grow exponentially whenever

$$\mu^2 < 2q\,|A|^2. \tag{44}$$

In order to observe this exponential growth numerically we need a more efficient

scheme than the one used in the previous section to solve (20). Using the midpoint rule we solve

$$\left(M+\frac{1}{2}rS\right)\mathbf{U}^{n+1}=\left(M-\frac{1}{2}rS\right)\mathbf{U}^{n}-\tau qM\mathbf{F}\left(\frac{\mathbf{U}^{n+1}+\mathbf{U}^{n}}{2}\right) \tag{45}$$

for $n=1, 2,\ldots$.

The nonlinear system of algebraic equation (45) was solved using a predictor–corrector procedure as in the previous section, but iterated to the desired accuracy. Thus, at each time step we used (37a) to provide an estimate $\mathbf{U}^{(1)}$ of $\mathbf{U}^{n+1}$ which was then iterated according to

$$\left(M+\frac{1}{2}rS\right)\mathbf{U}^{(k+1)}=\left(M-\frac{1}{2}rS\right)\mathbf{U}^{n}-\tau qM\mathbf{F}\left(\frac{\mathbf{U}^{(k)}+\mathbf{U}^{n}}{2}\right) \qquad k=1, 2,\ldots, m. \tag{46}$$

For this experiment we have found that 10 iterations ($m=10$) were sufficient.

The values of the parameters appearing in (43) were chosen to be: $A=0.5$; $a_1(0)=a_2(0)=0.1$. Furthermore $q=2$, 20 elements and periodic boundary conditions over one space period

$$-\pi/\mu \leqslant x \leqslant \pi/\mu$$

were used. For these values of the parameters, (44) becomes

$$\mu^2<1. \tag{47}$$

Three cases were investigated namely $\mu=1.1$; $\mu=1/\sqrt{2}$, and $\mu=0.4$. According to (47) the first choice does not allow exponential growth in the solution. This is clearly illustrated by Fig. 5. The choices $\mu=1/\sqrt{2}$ and $\mu=0.4$ are inside the stability limit (47) and the exponential growth in the solutions are shown in Figs. 6

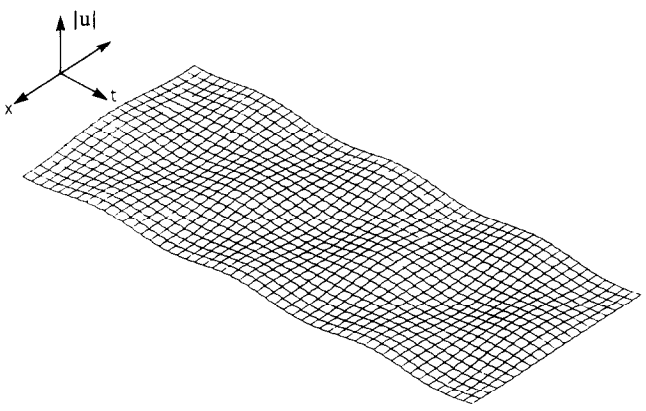

FIG. 5. Recurrence for $\mu=1.1$.

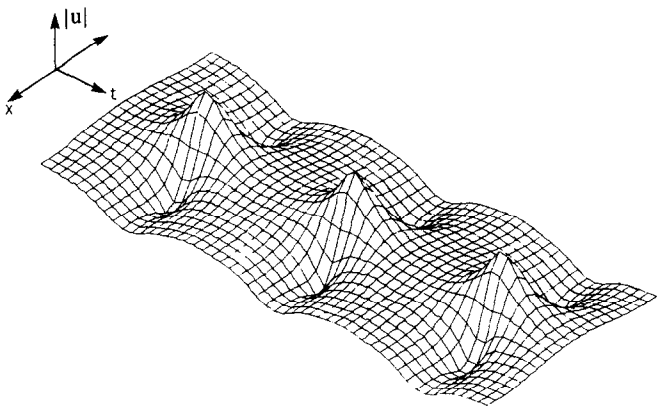

FIG. 6. Recurrence for $\mu = 1/\sqrt{2}$.

and 7, respectively. From these two figures a remarkable phenomenon is observed: The initial condition is periodically reconstructed even after fairly complex intermediate development, as in the case of Fig. 7. This phenomenon, which is not uncommon among nonlinear problems in general is known as recurrence and was first observed by Fermi, Pasta, and Ulam [7]. The connection between recurrence and the instability of the NLS was first pointed out by Yuen and Ferguson [24]. Incidentally, Yuen and Ferguson also gave numerical examples but used a numerical procedure entirely different from ours.

In order to explain the complex behaviour in the terms of Yuen and Ferguson and also to monitor the evolution of $a_1(t)$ and $a_2(t)$ appearing in (43b) the numerical solution at each time level t is written as

$$U_j(t) = \sum_{k=-N/2}^{N/2-1} \alpha_k(t) \exp(ik\mu x_j), \qquad j = -N/2, \ldots, N/2-1 \tag{48}$$

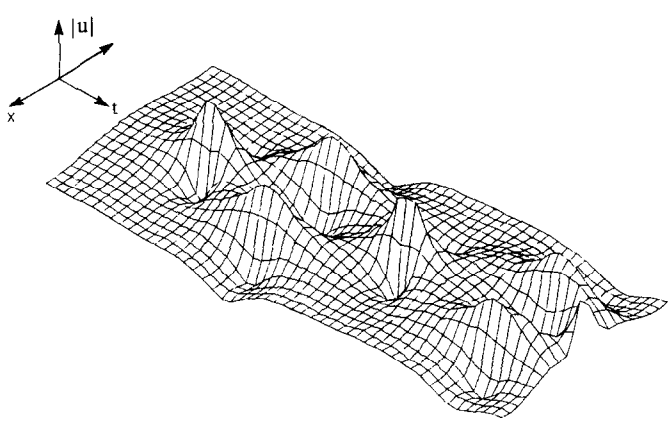

FIG. 7. Recurrence for $\mu = 0.4$.

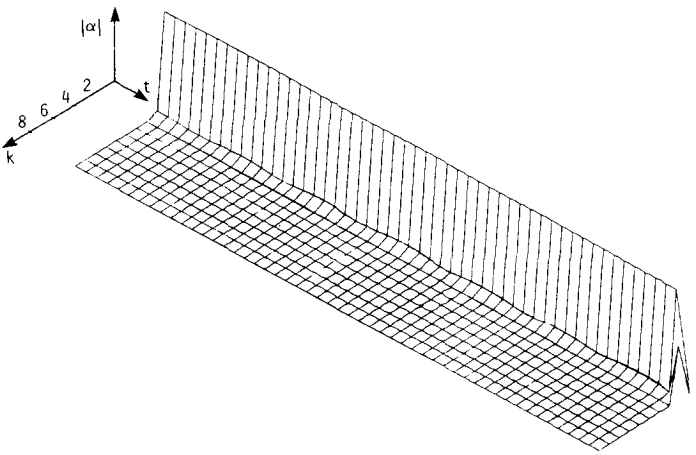

FIG. 8. Fourier transform for $\mu = 1.1$.

where N is the number of elements and

$$x_j = \frac{2\pi j}{\mu N}.$$

The α_k are evaluated by the fast Fourier transform. Initially (at $t = 0$), (48) consists of only the three modes α_0, α_1, and α_{-1} corresponding to A, Aa_1, and Aa_2 in (43), respectively, with most of the "energy" concentrated in the fundamental mode α_0. In the stable case, $\mu = 1.1$, we observe from Fig. 8 that this energy distribution remains fairly uniform with time. However, in the unstable cases, $\mu = 1/\sqrt{2}$ and $\mu = 0.4$, it is clear from Figs. 9 and 10 that energy is transferred to the higher modes.

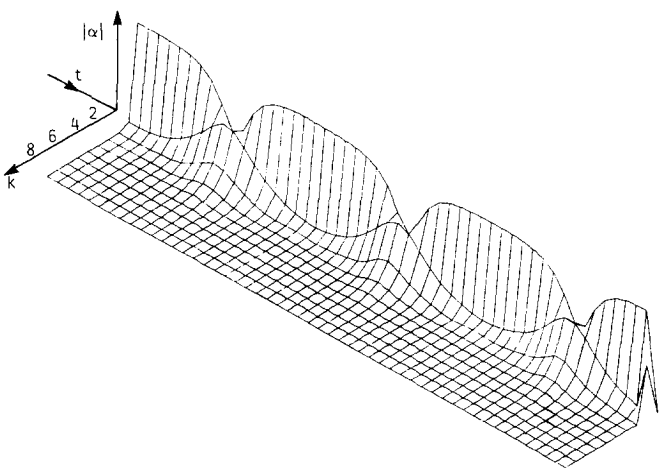

FIG. 9. Fourier transform for $\mu = 1/\sqrt{2}$.

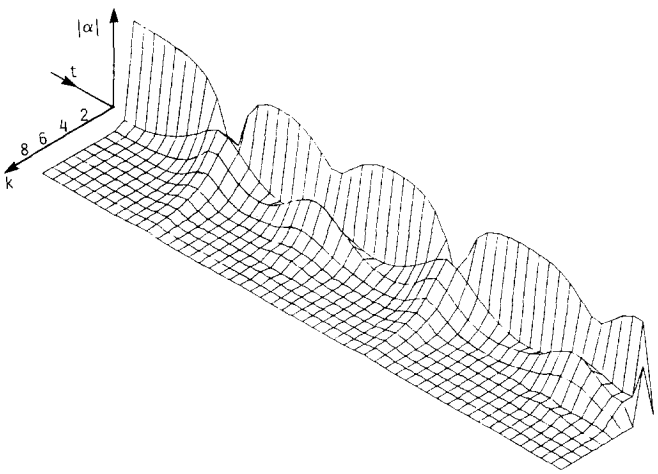

FIG. 10. Fourier transform for $\mu = 0.4$.

In the case of $\mu = 1/\sqrt{2}$, μ falls within the instability region given by (47) and α_1 starts to grow exponentially as predicted. However, after a certain time the energy is transferred back to the fundamental mode and the original distribution of energy is regained.

In the case of $\mu = 0.4$ energy is also transferred to the higher modes. However, since

$$2\mu = 0.8$$

μ and 2μ fall within the instability region and not only α_1 but also α_2 starts to grow exponentially. Since 2μ falls within the instability region the terms $\alpha_2(t)\exp(i2\mu x)$ and $\alpha_{-2}(t)\exp(-i2\mu x)$ appearing in (48) may be considered to be an unstable perturbation in the same sense as (43). In this case, however, the perturbation has period π/μ. Since we use periodic boundary conditions at $-\pi/\mu$ and π/μ, i.e., a period of $2\pi/\mu$, two peaks appear when α_2 becomes unstable. In general, M peaks will eventually appear, where

$$M = \text{Integer}(1/\mu)$$

i.e., M is the integer part of $1/\mu$.

Apparently, the unstable modes dominate in turn. For instance in Fig. 7 we see first one peak and then two peaks appearing. It is remarkable that the energy distribution between the various modes will eventually return almost exactly to the initial state.

8. Conclusions

In the preceding sections we have shown that the analytical instability properties of the nonlinear Schrödinger equation have an influence on the various discretisations. This is of special significance since analytical instability of the NLS is related to various important physical phenomena such as solitons or recurrence, the latter in periodic problems. These are precisely the phenomena that one would normally wish to observe by numerical means. This of course implies long time integrations whereas our analysis only holds for short times while the perturbations are still small. At least we have shown that the numerical schemes start off in the right way.

As far as the long time behaviour of the numerical methods is concerned, extreme care is necessary in order to obtain reasonable approximations. In the analytical case the instabilities are kept in check by the various conservation laws such as (16). Our numerical example seemingly indicates that numerical schemes that do not satisfy discrete analogues of these conservation laws are likely to behave badly in long-time integrations and that the solution may even become unbounded. This suggestion is investigated in more detail in a separate report (Herbst *et al.*, [12]). However, we did show our numerical schemes to be quite capable of approximating such a highly nonlinear phenomenon as recurrence.

Acknowledgments

This research was carried out at the University of Dundee, Scotland. Financial support from the CSIR, Pretoria and the University of the Orange Free State is gratefully acknowledged by B. M. Herbst and J. A. C. Weideman. We have benefitted from discussions with J. C. Eilbeck, D. F. Griffiths, and J. Ll. Morris.

References

1. T. B. Benjamin and J. E. Feir, *J. Fluid Mech.* **27** (1967), 417.
2. W. Briggs, A. C. Newell, and T. Sarie, *J. Comput. Phys.* **51** (1983), 83.
3. R. C. Y. Chin, G. W. Hedstrom, and K. E. Karlsson, *Math. Comp.* **33** (1979), 647.
4. I. Christie, D. F. Griffiths, A. R. Mitchell, and J. M. Sanz-Serna, *IMA J. Numer. Anal.* **1** (1981), 253.
5. M. Delfour, M. Fortin, and G. Payre, *J. Comp. Phys.* **44** (1981), 277.
6. R. K. Dodd, J. C. Eilbeck, J. D. Gibbon, and H. C. Morris, "Solitons and Nonlinear Wave Equations," Academic Press, London, 1982.
7. E. Fermi, J. Pasta, and S. Ulam, "Studies of Nonlinear Problems, I," reprinted in "Nonlinear Wave Motion," (A. C. Newell, Ed.), Amer. Math. Soc., Providence, R.I., 1974.
8. B. Fornberg, *Math. Comp.* **27** (1973), 45.
9. R. T. Glassey, *J. Math. Phys.* **18** (1977), 1794.
10. D. F. Griffiths, "The Stability of Finite Difference Approximations to Non-linear Partial Differential Equations," Report NA/51, University of Dundee, Scotland, 1981.
11. D. F. Griffiths, A. R. Mitchell, and J. Ll. Morris, *Comp. Meth. Appl. Mech. Engng.* **45** (1984), 177.

12. B. M. HERBST, A. R. MITCHELL, AND J. LL. MORRIS, *J. Comput. Phys.* **60** (1985).
13. P.-Y. KUO AND J. M. SANZ-SERNA, *IMA J. Numer. Anal.* **1** (1981), 215.
14. B. M. LAKE, H. C. YUEN, H. RUNGALDIER, AND W. E. FERGUSON, *J. Fluid Mech.* **83** (1977), 49.
15. B. M. LAKE AND H. C. YUEN, *J. Fluid Mech.* **83** (1977), 75.
16. A. R. MITCHELL AND J. LL. MORRIS, 1982, submitted for publication.
17. A. R. MITCHELL AND S. W. SCHOOMBIE, "Finite Element Studies of Solitons," Report NA/47, University of Dundee, Scotland, 1981.
18. J. M. SANZ-SERNA, *J. Comput. Phys.* **47** (1982), 199.
19. J. M. SANZ-SERNA AND V. S. MANORANJAN, *J. Comput. Phys.* **52** (1983), 273.
20. W. A. STRAUSS, *in* "Contemporary Developments in Continuum Mechanics and Partial Differential Equations" (G. M. de la Penha and L. A. Madeiros, Eds.), North–Holland, New York, 1978.
21. J. T. STUART AND R. C. DI PRIMA, *Proc. R. Soc. London A.* **362** (1978), 27.
22. G. B. WHITHAM, "Linear and Nonlinear Waves," Wiley, New York, 1974.
23. H. C. YUEN AND W. E. FERGUSON, *Phys. Fluids* **21** (1978), 1275.
24. H. C. YUEN AND B. M. LAKE, *Phys. Fluids* **18** (1975), 956.
25. V. E. ZAKHAROV AND A. B. SHABAT, *Sov. Phys.—JETP (Engl. Transl.)* **34** (1972), 62.